JOTCS A
Journal of the Turkish Chemical Society
Section: A
Chemistry
TURKISH CHEMICAL SOCIETY

# Removal of Malachite Green from Wastewaters by Bentonite-Based Photocatalytic Technology

**Kinyas Polat*** and **Muruvvet Yurdakoc**

Dokuz Eylul University, Faculty of Sciences, Department of Chemistry, Tinaztepe, 35390, Izmir, Turkey.

**Abstract:** $MgFe_2O_4$-B/$Ag_3VO_4$ visible light active photocatalyst was successfully synthesized for the photocatalytic decolorization of organic pollutants. Malachite green (MG) was selected as a model dye representing those pollutant chemicals. The catalyst was characterized by X-ray diffraction (XRD), scanning electron microscope (SEM) and energy dispersive X-ray spectroscopy (EDS). Malachite green (MG) decolorization was carried out by visible light irradiation of a 105 W tungsten light source. Decolorization yield and kinetic studies were traced by the help of a UV-Vis spectrophotometer. Kinetic model of decolorization was derived from Langmuir–Hinshelwood (L–H) model and found coherent to first order kinetics. Catalysis reaction showed high dependency on pH especially out of 5-7 range which gave high decolorization. Photocatalytic activity also depended on concentration with dual character in which high concentration hindered the light coming to catalyst surface but on the other hand it supported the activity by boosting the dark adsorption resulting in a decolorization time changing from 40 to 100 min. After the reaction was completed, powders of catalyst were effortlessly removed from the medium by a magnet bar. It was shown that $MgFe_2O_4$-B/$Ag_3VO_4$ photocatalyst has a potential to be simple and efficient alternative material for the removal pollution resources from wastewaters.

**Keywords:** Malachite green, photocatalyst, visible light active catalyst, decolorization, wastewater.

**Submitted:** February 13, 2019. **Accepted:** May 22, 2019.

**Cite this:** Polat K, Yurdakoc M. Removal of Malachite Green from Wastewaters by Bentonite-Based Photocatalytic Technology. JOTCSA. 2019;6(2):261–70.

**DOI:** https://dx.doi.org/10.18596/jotcsa.526822.

***Corresponding author. E-mail:** kinyas.polat@deu.edu.tr.

## INTRODUCTION

Industrial wastewaters containing hazardous dye molecules have detrimental consequences to human and animal life (1). Malachite green (MG) is one of those toxic dyes and is consist of N-methylated diaminotriphenylmethane. MG is heavily utilized for dying fabrics in textile industry and also used as a fungicide and a bactericide in aquatic industry. It is known that MG is responsible for hepatic toxicity, cancer, anemia, and thyroid tumors (2,3) and several studies were made to remove the MG from the wastewaters with photocatalytic technology (4,5,6) In finding effective ways to prevent the contamination of water effluents by these chemicals, important advancements have been made recently using photocatalytic technology that is being one of the most efficient means operating at mild conditions. Photocatalytic oxidation degrades the toxic molecules into nontoxic mineralized forms (7-10).

Photocatalyst materials are usually made from transition metal oxides such as $TiO_2$, ZnO, $BiPO_4$. $TiO_2$ is still the most widely investigated photocatalytic material up to now due to good performance, photostability, and low cost, but only active at UV region of the spectrum which is roughly 4% of the solar spectrum. This situation limits its effective usage (11,12,13). In order to utilize natural sunlight efficiently, it is necessary to design visible light sensitive photocatalysts.

Since $Ag_3VO_4$ emerged as a photocatalyst having activity towards visible light, it has attracted a lot of interest (14). $Ag_3VO_4$ has a narrowed band gap (15) suitable for efficient absorption of sunlight but charge carriers formed during excitation has small life-time. Therefore, produced electrons are captured by holes before the reduction reaction completely finished. Another drawback of $Ag_3VO_4$ is the low adsorptive capacity (16).

There are several efforts to increase the photocatalytic activity by making composites with mediators such as graphene oxide, $Co_3O_4$, and $Gd_2O_3$. These materials act in two ways, one is increasing the life time of charge carriers to suppress the recombination of electron and hole pairs, the other way is to create adsorption sides close to the catalyst active surface (17-21). In addition to activity enhancement issue, taking out of the catalyst from the aqueous solution without employing conventional expensive techniques is another important concept. For this purpose, magnetic $MgFe_2O_4$ nanoparticles are recently used for easy and fast separation (22,23).

Here, bentonite nanoparticles were incorporated to the $Ag_3VO_4$ photocatalyst to increase the photocatalytic performance. To the best of our knowledge this is the first study using bentonite as an adsorbent with $Ag_3VO_4$ formulations. Furthermore, magnetic $MgFe_2O_4$ nanoparticles were used for efficient removal of the catalyst by external magnetic field.

## MATERIALS AND METHODS

### Materials

$AgNO_3$ and $V_2O_5$ were purchased from Sigma Aldrich. $FeCl_3.6H_2O$, $FeCl_2.4H_2O$, $Mg(OAc)_2.4H_2O$, $NH_4OH$ (25 %) and sodium hydroxide were taken from Merck. Bentonite was brought from Edirne-Enez / Turkey region. Simulated wastewater was prepared with a mixture of sodium dodecyl sulfate (SDS), $NH_4NO_3$, NaCl, $NaHCO_3$, and grease at 100 ppm of each. All chemicals in the simulated wastewater were purchased from Merck.

### Preparation of the Photocatalyst

NaOH and $V_2O_5$ were stirred with a magnetic stirrer by 6:1 proportion in distilled water. By pouring the solution of $AgNO_3$, a yellow-orange precipitate was obtained. Half reactions of the synthesis can be written as follows;

$$V_2O_5 + 6OH^- \rightarrow 2VO_4^{3-} + 3\,H_2O$$
$$3Ag^+ + VO_4^{3-} \rightarrow Ag_3VO_4$$

The precipitate was left at room temperature for 24 h, cleaned thoroughly with deionized water and dried at 70 °C. Precipitate dying was done at 300 °C for 4 h (24). For $MgFe_2O_4$-Bentonite ($MgFe_2O_4$-B) nanoparticles, a definite amount of bentonite was added to the mixture of $FeCl_2.4H_2O$ and $FeCl_3.6H_2O$ in deionized water under nitrogen atmosphere. After 10 min,10 mL of $NH_4OH$ (25%) was added and mixed giving $Fe_3O_4$. Co-precipitation was achieved by drop by drop mixing of $Mg(OAc)_2.4H_2O$ to the suspension. $Mg(OH)_2$ was the resulting compound with the reaction 1 M aqueous NaOH. The powder was washed with deionized water, filtered, dried and calcined at 550 °C for 6.5 h (25). Finally, 0.5 g $Ag_3VO_4$ was mixed with 0.5 % $MgFe_2O_4$-B in an agate mortar for 30 min and calcined at 300 °C for 2 hours (26). The material was characterized by XRD for crystal structure analysis. The size and surface morphology examined by SEM.

### Photocatalytic performance

MG solution containing catalyst powders were irradiated by visible light produced from 105 W tungsten light source. MG content and the volume of the solution were $1\times10^{-5}$ M and 50 mL. Continuously stirred beaker was used to homogenize the solution during reaction. Samples were taken from the beaker at regular intervals and absorbance values were recorded at (615) nm wavelength by using a UV-visible spectrophotometer.

### Mechanism of Photocatalytic process

Formation of reactive species, caused by visible light as ·OH, HOO· is the main reason for decolorization or decomposing of MG. MG molecule is decomposed into harmless products. Commonly accepted mechanisms (27) can be written as follows;

$$Catalyst + h\gamma \rightarrow Catalyst\,(e_{CB}^- + h_{VB}^+)$$
$$H_2O + h_{VB}^+ \rightarrow HO\cdot + H^+$$
$$O_2 + e_{CB}^- \rightarrow O_2^{-\cdot}$$
$$O_2^{-\cdot} + H_2O \rightarrow H_2O_2$$
$$O_2^{-\cdot} + H^+ \rightarrow HOO\cdot$$
$$H_2O_2 \rightarrow 2HO\cdot$$
$$HO\cdot \text{ or } HOO\cdot + MB \rightarrow decolorization\ of\ MB$$

The reaction mechanism that converts MG into final products may be represented as in Figure 1.


**Figure 1.** Schematic demonstration of Malachite Green decolorization.

**Basics of kinetics in photocatalysis**

Heterogeneous photocatalysis generally conforms to the Langmuir–Hinshelwood (L–H) model. If the MB solution is not so concentrated, first order kinetic model is applied (27, 28). L-H kinetic expression can be formulized as in the equation 1.

$$r = \frac{dC}{dt} = \frac{kKC}{1+KC} \qquad \text{(Eq. 1)}$$

In the L-H equation, r is photocatalytic reaction rate, k is the intrinsic reactivity constant, K is the equilibrium adsorption constant, C is the reactant concentration. L-H expression can be written as in the form of basic first order kinetic equation for dilute solutions (1+KC roughly equals 1) as;

$$r = \frac{dC}{dt} = -k\,C \qquad \text{(Eq. 2)}$$

Using the integral function between the limits C and $C_0$ (beginning concentration) the equation 2 turns into the linear first order kinetic equation as follows;

$$\ln\left(\frac{C}{C_0}\right) = -k\,t \qquad \text{(Eq. 3)}$$

Where C is the concentration of dye at time t, k is the rate constant. A plot of $\ln(C/C_0)$ versus t results in a linear relationship, slope of which is the rate constant, k. Half-life ($t_{1/2}$) of the photocatalytic decolorization is calculated from the equation 4;

$$t_{1/2} = \frac{0{,}693}{k} \qquad \text{(Eq. 4)}$$

## RESULTS AND DISCUSSION

**XRD characterization**

XRD patterns of the catalyst's components were introduced in Figure 2. Monoclinic crystalline structure was observed for $Ag_3VO_4$ due to the diffraction peaks' positions that were collected at the 2θ values as 19.1°, 30.5°, 32.5°, 35.3°, 36.1°, 39.2, 41.3°, 51.2°, 54.0° (24, 26, 29, 30) which is matched to JCPDS No. 43-0542. Absorbance at 32.5° belongs to the impurity of $Ag_2O$ (JCPDS No: 41-1104). Usually the peaks were sharp and narrow revealing that the sample (Figure 2), $MgFe_2O_4$-B/$Ag_3VO_4$ was almost perfect crystalline. 2θ values collected at 27.5 °, 33 °, 35.5°, 43.1°, 49.2 °, 54.0 °, 63.2° correspond to cubic structure of $MgFe_2O_4$-B (JCPDS card No. 36-0398) (25). XRD pattern of $MgFe_2O_4$-B was hindered by $Ag_3VO_4$ pattern for being the most abundant component of the catalyst formulation. The peak intensities of $Ag_3VO_4$ increased by 60 % due to the additional calcination carried out for fusing of $MgFe_2O_4$-B into $Ag_3VO_4$ for obtaining resulting catalyst $MgFe_2O_4$-B/$Ag_3VO_4$ with an enhancement in crystal regularity.

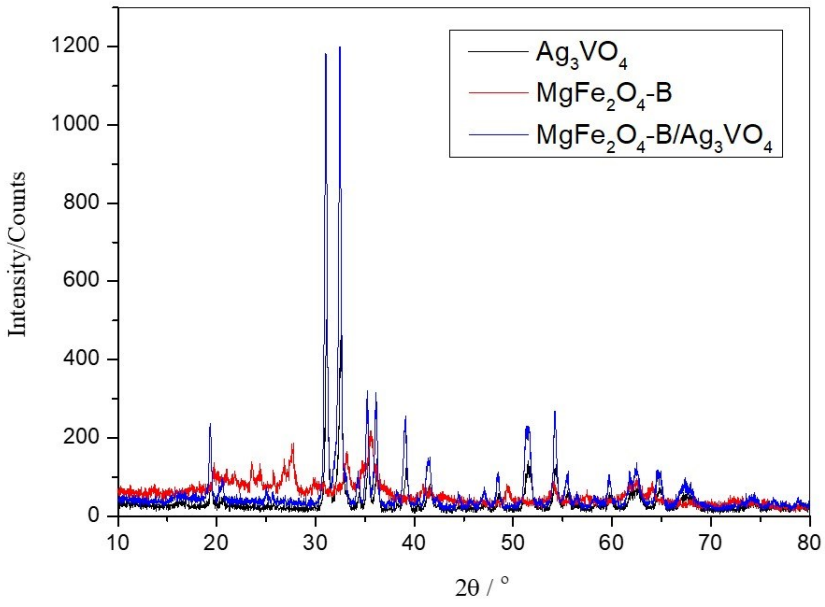


**Figure 2.** XRD spectrum of $MgFe_2O_4$-B/$Ag_3VO_4$

**Analyses by SEM and EDS**

SEM image of $MgFe_2O_4$-B/$Ag_3VO_4$ collected through 10.00 kX magnification with 5.00 kV beam voltage is given in Figure 3. Particle and void dimensions demonstrates a distribution from 0,1 to 5 μm. Elemental analysis determined by EDS is in harmony with the chemical structure of the catalyst. Theoretically, silver (Ag), vanadium (V) and oxygen (O) have to exist in the molecular formula with 73.75, 11.61 and 14.59 % respectively. EDS analysis verified their related amounts as 73.91, 12.28 and 13.78. Therefore, the molecular formula was determined to be $Ag_{3.01}V_{1.06}O_{3.77}$ which is almost the same with $Ag_3VO_4$. The smallest component, $MgFe_2O_4$-B (0.5 %) of the catalyst could not be proved by EDS due to the complete confinement in $Ag_3VO_4$ crystal structure.

**Photocatalysis of Malachite Green**

MG photocatalysis by $MgFe_2O_4$-B/$Ag_3VO_4$ photocatalyst was carried out in the existence of visible photons coming from 105 W tungsten light source. Dye concentration were measured at several time intervals. The UV-Vis spectrophotometer was used to monitor the residual concentration of MG at each interval at 615 nm. The initial MG concentration was $1\times10^{-5}$ M. The catalyst weight was 0.1 g. In order to differentiate the MG photolysis from the photocatalysis, MG decolorization which stems only from the light source (without catalysis) are also measured (Figure 4) and it was observed that MG is a stable dye under experimental conditions to the photolysis. Therefore, recorded decolorization is due to only photodecolorization. It is also seen that photocatalytic reaction due to $MgFe_2O_4$-B/$Ag_3VO_4$ efficiently decreases the MG dye concentration in the solution. The effect of dye concentration on photocatalytic decolorization was examined and the data was collected in the graph which is given in Figure 5. To clearly explain the concentration effect, there are two fact observed to be mentioned. Firstly, as the concentration of dye increases dark adsorption of the catalyst increases which reduce the amount of dye that must be removed when the light source is opened. Secondly as the concentration decreases dark adsorption decreases accordingly and the amount of dye that has to be removed remains as what was roughly the dye concentration is in the solution. This situation demonstrates that the process of dye adsorption is mass-transfer controlled. This means that at lower dye concentration photocatalytic activity reflects the real performance of the catalysis when exposed to visible light. On the other hand, at high concentration dark adsorption supports the photocatalytic activity by simply creating pre-concentrated sides near the active points of catalyst. In Figure 5, the reason for the higher photocatalytic activity observed for $2\times10^{-5}$ M solution than $1\times10^{-5}$ M is this fact in which dark adsorption over-supports the photocatalytic activity. However, the time required for complete decolorization of higher concentrations ($1.5\times10^{-5}$ and $2\times10^{-5}$M), which is nearly 100 min, does not decrease when compared to the low concentration ($1\times10^{-5}$ M) of 40 min. The fact behind this

observation is the transmittance of the solution that is very low at higher concentrations resulting in decreased photocatalytic activity. Adsorption values of the catalyst particles at the dark for 1 × $10^{-5}$ M, 1.5 × $10^{-5}$ M, 2 × $10^{-5}$ M and for simulated sample concentrations were found as 35.02, 50.86, 71.57 and 66.84 % respectively, dropped from the photocatalytically decreased amounts and not included in Figure 5.

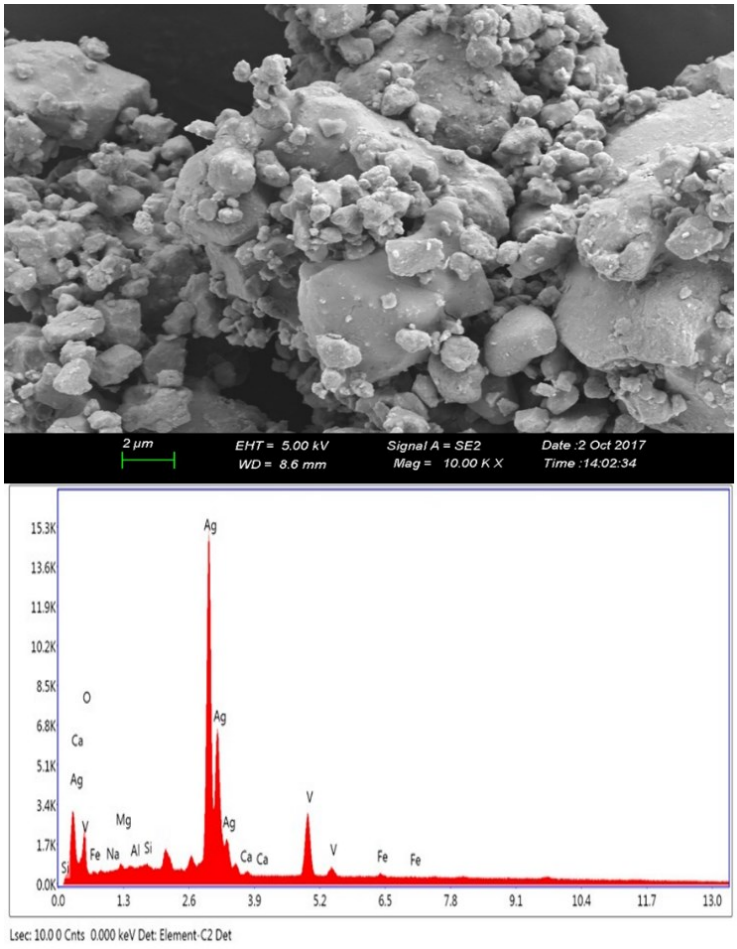


**Figure 3.** SEM image and EDS spectrum for the $MgFe_2O_4$-B/$Ag_3VO_4$ photocatalyst.

This study demonstrated that solution pH value has an enormous effect on decolorization. At pH ranges above 7 and below 5 decolorization take places very rapid not enabling the proper kinetic study of the photocatalytic process however this situation is an advantage for the factories having highly basic and acidic wastewater disposals. Between these two ranges kinetic studies of the decolorization can be done appropriately and elimination of the wastewater takes 40 min to 100 min depending on the concentration of the dye. A simulated wastewater was also tried to foresee the performance in real conditions. It was observed that dark adsorption of the catalyst was 58 % and total decolorization of the sample finished at 70 min in case of simulated wastewater.

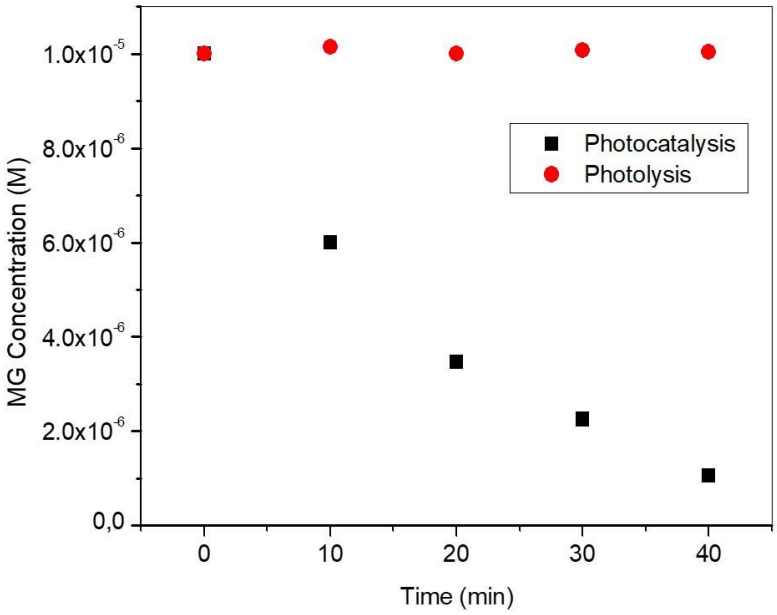


**Figure 4.** Effect of irradiation time on MG decolorization with $MgFe_2O_4$-B/$Ag_3VO_4$.

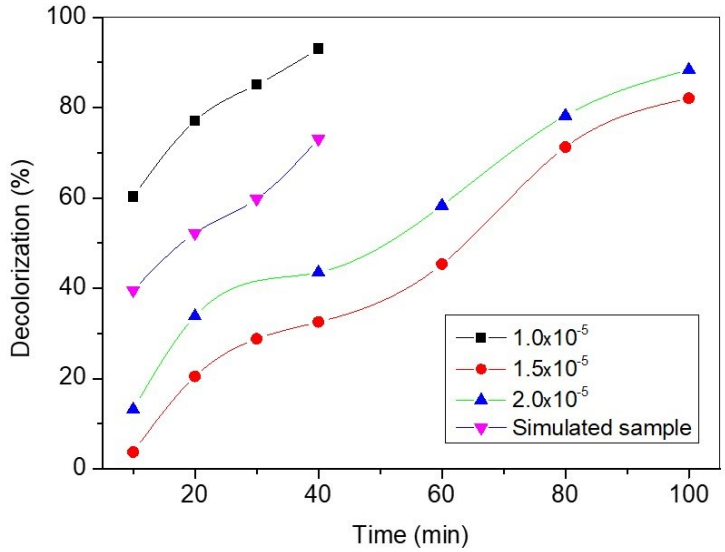


**Figure 5.** Effect of concentration of MG on decolorization.

First order kinetics was encountered as seen from the Figure 6. Rate constant k was obtained from the slope as 0.0542 $min^{-1}$. Related half life time at which MG concentration decreases to half of the initial is 12.8 min.

The effect of bentonite was identified by examining neat $Ag_3VO_4$. MG concentration versus time plot was given in Figure 7. It is seen that MG photocatalysis with $Ag_3VO_4$ takes approximately 65 min more than that of $MgFe_2O_4$-B/$Ag_3VO_4$ when Figure 4 and 7 are compared. Rate constant of the decolorization with $Ag_3VO_4$ was 0.01577 $min^{-1}$. Half-life was 43.9 min (Figure 8).

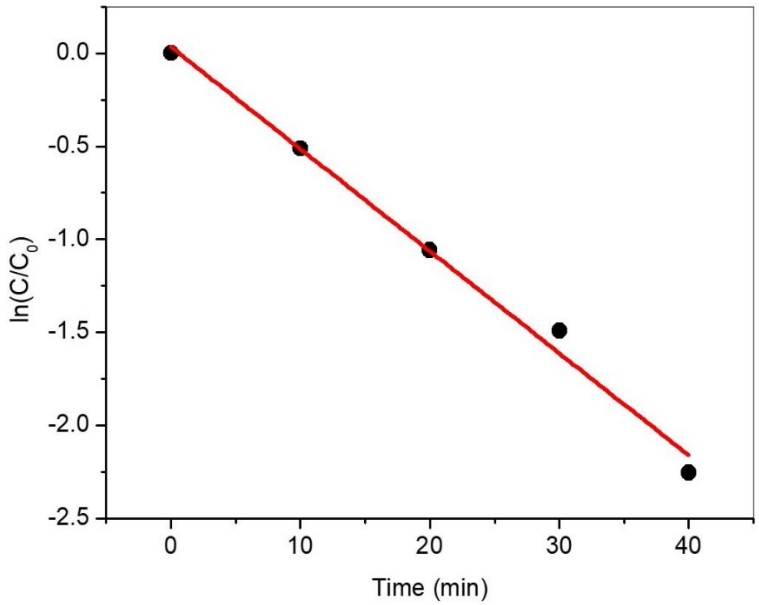


**Figure 6.** First order kinetic fitting for MG decolorization with $MgFe_2O_4$-B/$Ag_3VO_4$.

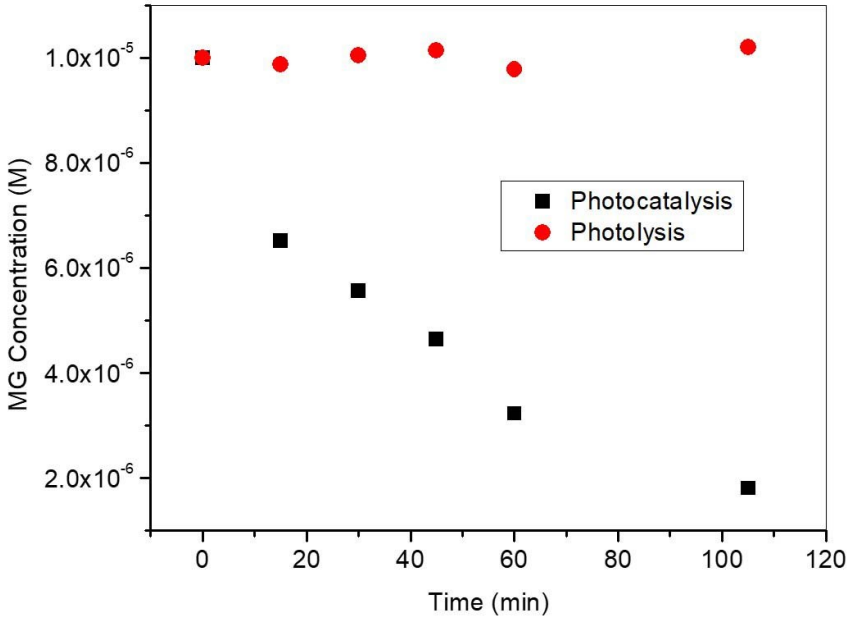


**Figure 7.** Concentration decrease of MG upon irradiation time with $Ag_3VO_4$ catalyst.

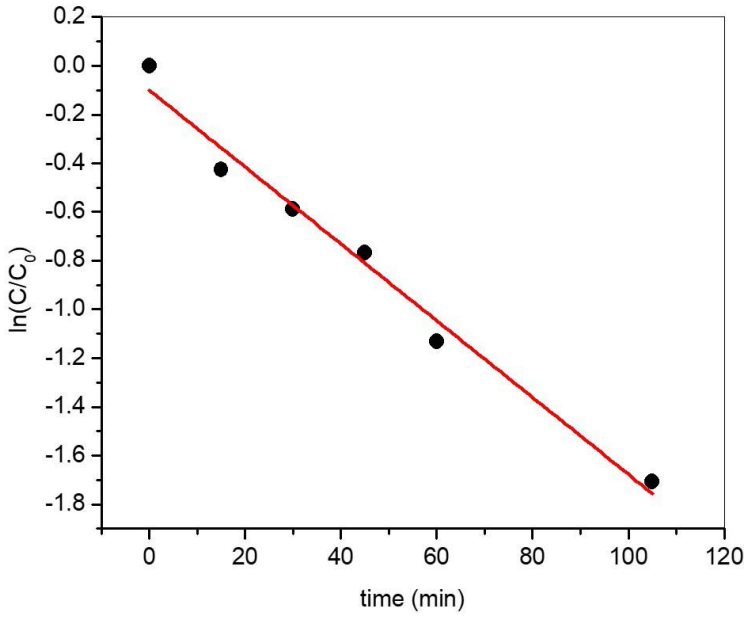


**Figure 8.** First order kinetic model fitting to MG decolorization with $Ag_3VO_4$ catalyst.

From the decolorization half-lives which are 12.8 min for $MgFe_2O_4$-B/$Ag_3VO_4$ and 43.9 min for $Ag_3VO_4$, incorporating of bentonite particles to the $Ag_3VO_4$ raised the photocatalytic activity almost 3.4 times when compared to pure $Ag_3VO_4$. This result can be ascribed to the adsorption by bentonite and hence forming dye reservoirs adjacent to the catalyst surface which accordingly promotes the rate of reaction (20). A photograph photo-catalytically degraded MG aqueous solution is introduced in Figure 9.

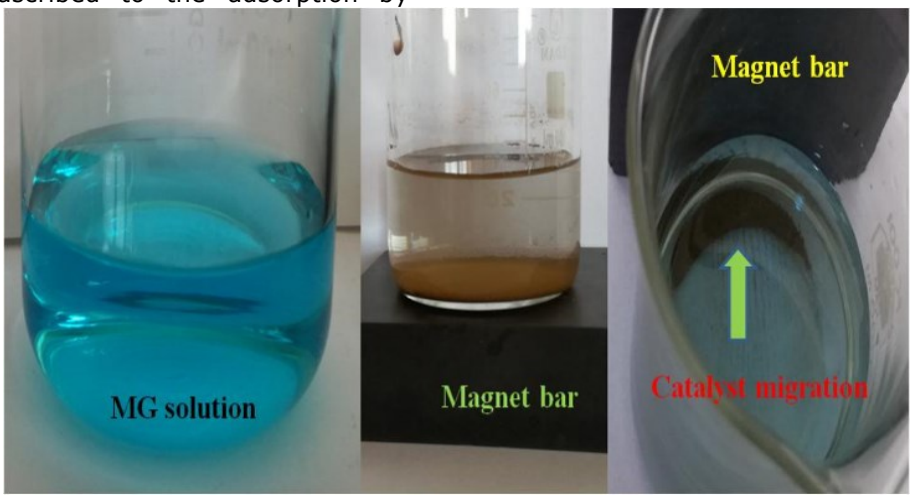


**Figure 9.** Photograph of the MG decolorization and magnetic collection of $MgFe_2O_4$-B/$Ag_3VO_4$ particles

From the photograph, catalyst particles containing $MgFe_2O_4$ are pulled towards the magnet after the reaction without needing ineffective conventional separation techniques. Recovery efficiency from reaction medium by means of a magnetic bar was found as 93% after three times of reuse. To determine the recovery efficiency, catalyst particles collected by magnetic bar, washed, dried at 90℃ for six hours and weighed. The ratio of the dried particles to the initial amount was evaluated as recovery efficiency for the material. Recovery efficiency was calculated according to the equation 5;

$$Recovery\ efficiency\ \% = \frac{W_e}{W_i} x100 \qquad \text{(Eq. 5)}$$

In the equation, $W_e$ is the average of residual catalyst after recovery. $W_i$ is the weight of initial catalyst.

## CONCLUSIONS

In this study, $MgFe_2O_4$-B/$Ag_3VO_4$ were synthesized as a visible region sensitive photocatalyst and its activity monitored by MG decolorization under visible light irradiation emitted from a 105 W tungsten light bulb. MG

concentration drop to half of its starting concentration at 12.8 min with a rate constant 0.0542 $min^{-1}$ in the case of $MgFe_2O_4$-B/$Ag_3VO_4$ catalyst. $Ag_3VO_4$ activity was also measured and MG concentration was found to be decreased to its half at 43.9 min and corresponding rate constant was 0.01577 $min^{-1}$. It was successfully demonstrated that bentonite addition amplified the photocatalytic activity of $Ag_3VO_4$ almost 3.4 times. Reaction kinetics were in harmony with first order kinetic model. A magnificent rate of decolorization occurred out of 5-7 pH range and color of the dye was immediately diminished. Photocatalysis reaction was so fast at high base or acid concentrations. Within this range a reasonable rate of decolorization at which physicochemical kinetic studies can be made was observed. Eventually, depending on the acidity of the waste effluents suitable decolorization rate could be obtained from 40 min to 100 min. A simulated wastewater also tested and showed that 70 min was enough to totally eliminate the color. Concentration of the dye was effected in two aspects on the decolorization by either supporting or hindering the performance. High concentration was the reason of activity decrease due to the low transparency but at the same time it was an activity supporter through an increased dark adsorption. Magnetic $MgFe_2O_4$ particles also worked well in removing catalyst particles away from the aqueous solution by magnet bar with a recovery efficiency of 93%.

**ACKNOWLEDGEMENTS**

The authors would like to thank to the Research foundation of Dokuz Eylul University (Project 2018.KB.FEN.011) for the financial support.

**REFERENCES**

1. McManamon C, O'Connell J, Delaney P, Rasappa S, Holmes JD, Morris MA. A facile route to synthesis of S-doped TiO2 nanoparticles for photocatalytic activity. J Mol Catal A-Chem. 2015;406:51–7.

2. Malathy P, Vignesh K, Rajarajan M, Suganthi A. Enhanced photocatalytic performance of transition metal doped Bi2O3 nanoparticles under visible light irradiation. Ceram Int. 2014;40(1, Part A):101–7.

3. Srivastava S, Sinha R, Roy D. Toxicological effects of malachite green. Aquat Toxicol. 2004;66(3):319–29.

4. Pare B, Sarwan B, Jonnalagadda S B. Photocatalytic mineralization study of malachite green on the surface of Mn-doped BiOCl activated by visible light under ambient condition. Appl Surf Sci. 2011;258(1):247-253.

5. Liu Y, Ohko Y, Zhang R, Yang Y,Zhang Z. Degradation of malachite green on Pd/WO3 photocatalysts under simulated solar light. J Hazard Mater. 2010;184(1-3):386-391.

6. Saikia L, Bhuyan D, Saikia M, Malakar B, Dutta DK,Sengupta P. Photocatalytic performance of ZnO nanomaterials for self sensitized degradation of malachite green dye under solar light. Appl Catal A:Gen. 2015;490:42-49.

7. Sturini M, Speltini A, Maraschi F, Pretali L, Profumo A, Fasani E, et al. Photodegradation of fluoroquinolones in surface water and antimicrobial activity of the photoproducts. Water Res. 2012;46(17):5575–82.

8. Lin G, Zheng J, Xu R. Template-Free Synthesis of Uniform CdS Hollow Nanospheres and Their Photocatalytic Activities. J Phys Chem C. 2008;112(19):7363–70.

9. Song S, Cheng B, Wu N, Meng A, Cao S, Yu J. Structure effect of graphene on the photocatalytic performance of plasmonic Ag/Ag2CO3-rGO for photocatalytic elimination of pollutants. Appl Catal B-Environ. 2016;181:71–8.

10. Jin Z, Murakami N, Tsubota T, Ohno T. Complete oxidation of acetaldehyde over a composite photocatalyst of graphitic carbon nitride and tungsten(VI) oxide under visible-light irradiation. Appl Catal B-Environ. 2014;150–151:479–85.

11. Liu Y, Yao W, Liu D, Zong R, Zhang M, Ma X, et al. Enhancement of visible light mineralization ability and photocatalytic activity of BiPO4/BiOI. Appl Catal B-Environ. 2015;163:547–53.

12. Abbasi A, Ghanbari D, Salavati-Niasari M, Hamadanian M. Photo-degradation of methylene blue: photocatalyst and magnetic investigation of Fe2O3–TiO2 nanoparticles and nanocomposites. J Mater Sci: Mater Electron. 2016;27(5):4800–9.

13. Tao X, Hong Q, Xu T, Liao F. Highly efficient photocatalytic performance of graphene–Ag3VO4 composites. J Mater Sci: Mater Electron. 2014;25(8):3480–5.

14. Lee KM, Lai CW, Ngai KS, Juan JC. Recent developments of zinc oxide based photocatalyst in water treatment technology: A review. Water Res. 2016;88:428–48.

15. Padervand M. Visible-light photoactive Ag–AgBr/α-Ag3VO4 nanostructures prepared in a water-soluble ionic liquid for degradation of

wastewater. Appl Nanosci. 2016;6(8):1119–26.

16. Wang S, Guan Y, Wang L, Zhao W, He H, Xiao J, Sun C. Fabrication of a novel bifunctional material of BiOI/Ag3VO4 with high adsorption–photocatalysis for efficient treatment of dye wastewater. Appl Catal B-Environ. 2015;168:448-457.

17. Bhunia SK, Jana NR. Reduced Graphene Oxide-Silver Nanoparticle Composite as Visible Light Photocatalyst for Degradation of Colorless Endocrine Disruptors. ACS Appl Mater Interfaces. 2014;6(22):20085–92.

18. Zhang L, He Y, Ye P, Qin W, Wu Y, Wu T. Enhanced photodegradation activity of Rhodamine B by Co3O4/Ag3VO4 under visible light irriadiation. Materials Science and Engineering: B. 2013;178(1):45–52.

19. Sun G, Xu H, Li H, Shu H, Liu C, Zhang Q. Fabrication and characterization of visible-light-induced photocatalyst Gd2O3/Ag3VO4. Reac Kinet Mech Cat. 2010;99(2):471–84.

20. Ren J, Wu Y, Dai Y, Sha D, Pan J, Chen M, et al. Preparation and characterization of graphitic C3N4/Ag3VO4 with excellent photocatalytic performance under visible light irradiation. J Mater Sci: Mater Electron. 2017;28(1):641–51.

21. Anderson C, Bard AJ. Improved Photocatalytic Activity and Characterization of Mixed TiO2/SiO2 and TiO2/Al2O3 Materials. J Phys Chem B. 1997;101(14):2611–6.

22. Arshadnia I, Movahedi M, Rasouli N. MgFe2O4 and MgFe2O4/ZnFe2O4 coated with polyaniline as a magnetically separable photocatalyst for removal of a two dye mixture in aqueous solution. Res Chem Intermed. 2017;43(8):4459–74.

23. Nabiyouni G, Ghanbari D, Ghasemi J, Yousofnejad A. Microwave-assisted synthesis of MgFe2O4-ZnO nanocomposite and its photo-catalyst investigation in methyl orange degradation. Journal of Nanostructures. 2015;5(3):289–295.

24. Hu X, Hu C. Preparation and visible-light photocatalytic activity of Ag 3VO 4 powders. Journal of Solid State Chemistry France. 2007;180:725–32.

25. Sheykhan M, Mohammadnejad H, Akbari J, Heydari A. Superparamagnetic magnesium ferrite nanoparticles: a magnetically reusable and clean heterogeneous catalyst. Tetrahedron Lett. 2012;53(24):2959–64.

26. Zhang L, He Y, Ye P, Qin W, Wu Y, Wu T. Enhanced photodegradation activity of Rhodamine B by Co3O4/Ag3VO4 under visible light irriadiation. Mater Sci Eng B. 2013;178(1):45–52.

27. Phaltane SA, Vanalakar SA, Bhat TS, Patil PS, Sartale SD, Kadam LD. Photocatalytic degradation of methylene blue by hydrothermally synthesized CZTS nanoparticles. J Mater Sci: Mater Electron. 2017;28(11):8186–91.

28. Mondal S, Reyes MEDA, Pal U. Plasmon induced enhanced photocatalytic activity of gold loaded hydroxyapatite nanoparticles for methylene blue degradation under visible light. RSC Adv. 2017;7(14):8633–45.

29. Sivakumar V, Suresh R, Giribabu K, Narayanan V. AgVO3 nanorods: Synthesis, characterization and visible light photocatalytic activity. Solid State Sci. 2015;39:34–9

30. Li Y-CM, Tsai R-H, Huang C-M. Preparation of nano-sized silver vanadates: characterization and photocatalytic activity. Proceedings of the Institution of Mechanical Engineers, Part N: Journal of Nanoengineering and Nanosystems. 2012;226(1):35–8.